

The development of an implicit full f method for electromagnetic particle simulations of Alfvén waves and energetic particle physics

Z. Lu, G. Meng, M. Hoelzl, Ph. Lauber

Acknowledge: A. Mishchenko, G. Huysmans, K. Kormann, A. Bottino, J. Chen,
T. Hayward-Schneider, B. Sturdevant, X. Wang and F. Zonca, NUMKIN2019,

EUROfusion Enabling Research Projects WP19-ER /ENEA-05 (PI: Zonca) and WP19-ER/MPG-03 (PI: Hoelzl)

NUMKIN workshop, 19th-23rd October, 2020



Outline

- Background and motivation
- Focus of this work
 - Full f electromagnetic simulation and TRIMEG development
- From “particle enslavement” to “moment enslavement”
 - One dimensional model of shear Alfvén wave
 - Implicit scheme with “moment enslavement”
- Simulation of Alfvén waves in tokamak plasmas
 - Gyrokinetic equation and conservation properties
 - The mixed explicit-implicit scheme for electromagnetic simulations
 - Alfvén and EP simulations of ITPA case
- Conclusion and outlook, short messages

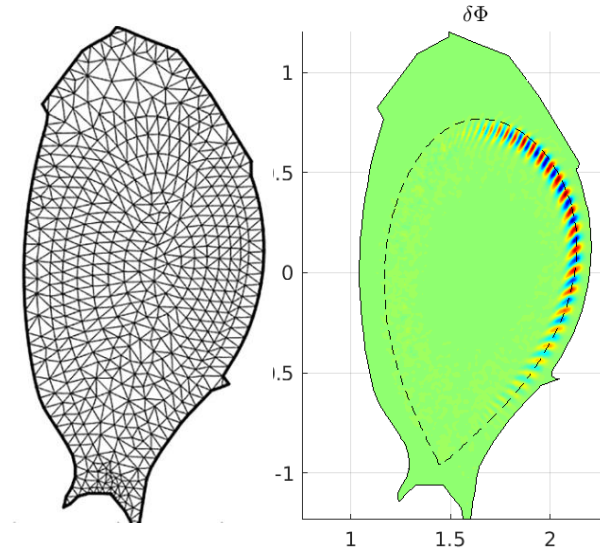
Background and motivation

- Early gyrokinetic PIC codes have adopted explicit δf as the main scheme
 - GYGLES, GTC, GTS, GEM, (ORB5) ...
- **Full f implicit scheme** enables studies of specific physics problems
 - Particle/heat/momentum source and sink
 - Significant profile change during simulation (flux driven simulations)
 - (Semi) implicit scheme or/and full f scheme have attracted numerous efforts
[Kleiber POP16, EUTERPE&ORB5, GEMPIC, GENE, ELMFIRE, XGC, ECSIM ...]
- Implicit scheme has advantages in conservation properties, large Δt but...
 - For a system with N_G field grids and N_p particles, the computational cost is too high
 - A direct implicit solver requires solving a linear system with $\text{DOF} = N_G + N_p$. Matrix size is $(N_G + N_p)^2$.
 - One possible solution: “particle enslavement” [Chen, et al, J. Comput. Phys. 230 (2011) 7018]
 - Particles (x, v) represented as functions of field $F(x)$ \rightarrow DOF reduced to N_G
 - The development of the implicit full f scheme for Alfvén wave/energetic particle physics has not been reported (physics motivation of this work)

Focus of this work

- This work: implementation in **tokamak plasmas**
 - Focus on **Darwin model**, instead of Vlasov-Maxwell (e.g., GEMPIC)
 - Focus on Alfvén modes, kinetic electron, realistic β/m_e
 - Derive the equations for **FEM** particle implicit scheme, useful for **TRIMEG** and also other codes (not FEM in [G. Chen 2011])
- Specific issues to be addressed in this work
 - What's the **minimum cost** of implicit scheme, especially when field **DOF is $>10^5$** (typical DOF in unstructured mesh FEM solver)?
*[Z.X. Lu et al, *Phys. Plasmas*, [26, 122503 \(2019\)](#)]*
 - Is the implicit scheme useful for mitigating “**cancellation problem**” or for simulations with **realistic ion to electron mass ratio**?
 - What are the technical **pros and cons** of the fully implicit scheme?
 - Any reasonable balance point between physics studies and numerical capabilities?

ITG mode, NLED equilibrium (ψ), analytical n, T profiles



Previous **TRIMEG** version: electrostatic, δf , mixed PIC-PIF, unstructured mesh, FEM. [Z.X. Lu, Ph. Lauber, T. Hayward-Schneider, A. Bottino, M. Hoelzl, *Phys. Plasmas*, [26, 122503 \(2019\)](#)]

References

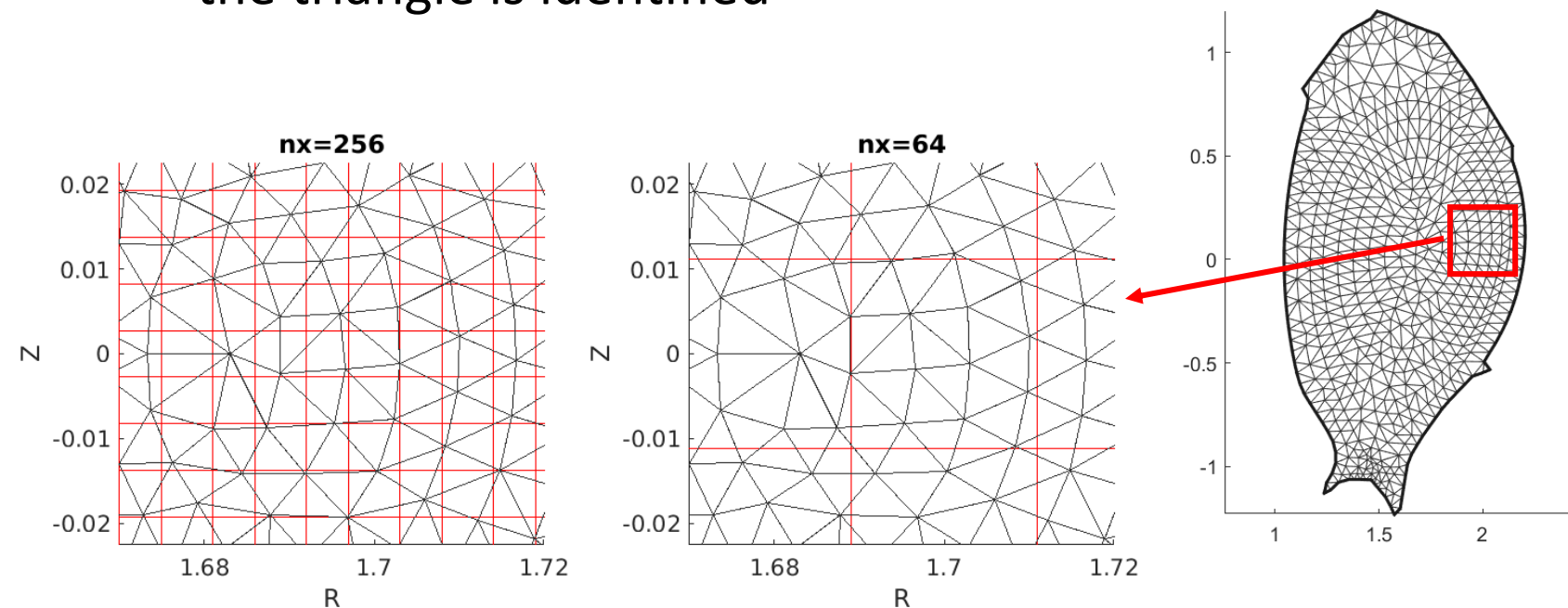
1. W. Lee, Phys. Fluids 26, 556 (1983)
2. Z. Lin, T. S. Hahm, W. Lee, W. M. Tang, and R. B. White, Science 281, 1835 (1998)
3. W.X. Wang, T.S. Hahm, W. W. Lee, G. Rewoldt, J. Manickam, W. M. Tang, *Physics of plasmas*, 14(7), 072306 (2007).
4. B. I. Cohen, A. B. Langdon, D. W. Hewett, and R. J. Procassini, J. Comput. Phys. 81, 151 (1989)
5. B. Sturdevant, S.-H. Ku, C. Chang, R. Hager, L. Chacon, and G. Chen, Bulletin of the American Physical Society (2019)
6. C. Chang, S. Ku, G. Tynan, R. Hager, R. Churchill, I. Cziegler, M. Greenwald, A. Hubbard, and J. Hughes, Phys. Rev. Lett. 118, 175001 (2017)
7. G. Chen, L. Chacon, and D. C. Barnes, J. Comput. Phys. 230, 7018 (2011)
8. J. A. Heikkinen, S. J. Janhunen, T. P. Kiviniemi, and F. Ogando, J. Comput. Phys. 227, 5582 (2008)
9. R. Hatzky, Journal of Computational Physics 225, 568–590 (2007)
10. A. Mishchenko, A. Bottino, A. Biancalani, R. Hatzky, T. Hayward-Schneider, N. Ohana, E. Lanti, S. Brunner, L. Villard, M. Borchardt, et al., Comput. Phys. Commun. 238, 194 (2019)
11. R. Kleiber, R. Hatzky, A. Könies, A. Mishchenko, and E. Sonnendrücker, Phys. Plasmas 23, 032501 (2016)
12. E. Lanti, N. Ohana, N. Tronko, T. Hayward-Schneider, A. Bottino, B. McMillan, A. Mishchenko, A. Scheinberg, A. Biancalani, P. Angelino, et al., Comput. Phys. Commun. , 107072 (2019)
13. A. Könies, S. Briguglio, N. Gorelenkov, T. Feh´er, M. Isaev, P. Lauber, A. Mishchenko, D. Spong, Y. Todo, W. Cooper, et al., Nucl. Fusion 58, 126027 (2018)
14. A. Biancalani, A. Bottino, M. Cole, C. Di Troia, P. Lauber, A. Mishchenko, B. Scott, and F. Zonca, Plasma Phys. Controlled Fusion 59, 054004 (2017)
15. M. Kraus, K. Kormann, P.J. Morrison, *Journal of Plasma Physics* 83.4 (2017).
16. K. Kormann, E. Sonnendrücker, Journal of Computational Physics, 109890 (2020)
17. T. Hayward-Schneider, Thesis “Global nonlinear fully gyrokinetic and hybrid treatments of Alfvénic instabilities in ITER” (2020)
18. Jakob Ameres, Ph.D thesis, Stochastic and Spectral Particle Methods for Plasma Physics (2017)
19. S. Taimourzadeh, E. M. Bass, Y. Chen, C. Collins, N. N. Gorelenkov, A. Konies, Z. X. Lu, D. A. Spong, Y. Todo, M. E. Austin, J. Bao, A. Biancalani, M. Borchardt, A. Bottino, W. W. Heidbrink, Z. Lin, R. Kleiber, A. Mishchenko, L. Shi, J. Varela, R. E. Waltz, G. Yu, W. L. Zhang, and Y. Zhu, *Nuclear Fusion*, [59 \(6\), 066006 \(2019\)](#)
20. W.X. Wang, S. Ethier, Y. Ren, S. Kaye, J. Chen, E. Startsev, Z.X. Lu, *Nuclear Fusion* , [55 \(12\), 122001 \(2015\)](#)
21. Z.X. Lu, W.X. Wang, P.H. Diamond, G. Tynan, S. Ethier, J. Chen, C. Gao, J.E. Rice, *Nuclear Fusion* , [55 \(9\), 093012 \(2015\)](#)
22. L. Chen and F. Zonca, Rev. Mod. Phys. 88, 015008 (2016)
23. Zonca, Phys. Fluids B 5, 3668 (1993);
24. Z.X. Lu, F. Zonca, A. Cardinali, *Phys. Plasmas*, [19 \(4\), 042104 \(2012\)](#)
25. Z.X. Lu, P. Lauber, T. Hayward-Schneider, A. Bottino, and M. Hoelzl, Phys. Plasmas 26, 122503 (2019)
26. Z.X. Lu, G. Meng, M. Hoelzl, Ph. Lauber, *arXiv preprint arXiv:2007.06935* (2020)

Recap: previous electrostatic δf version of TRIMEG

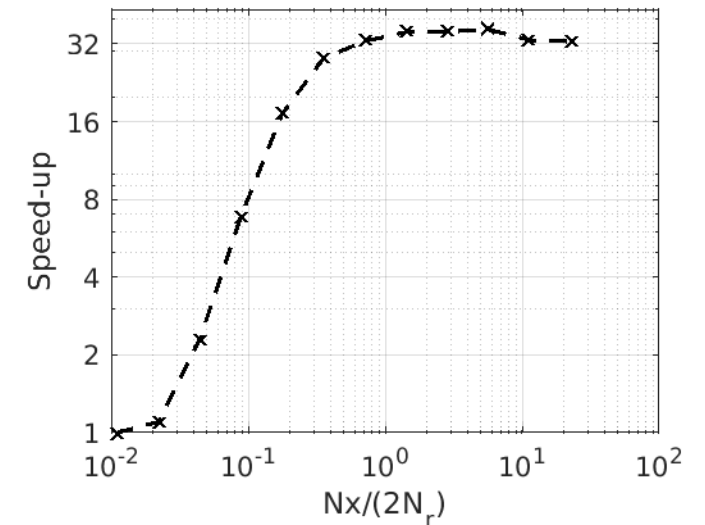
- TRIMEG: TRIangular MESH based Gyrokinetics
[Z.X. Lu, Ph. Lauber, T. Hayward-Schneider, A. Bottino, M. Hoelzl, *Phys. Plasmas* , [26, 122503 \(2019\)](#)]
- Coordinates (R, ϕ, Z) used in field & particle equations
- ψ used for mesh generation
- 2D Unstructured meshes & FEM in (R, Z) plane FEM solver in (ψ, θ) in GTS
- δf method, Particle-in-cell in (R, Z) , particle-in-Fourier along ϕ (mixed PIF-PIC)
PIF in [Ameres, PhD thesis 2017]
- Simplifications in ITG simulation
 - Adiabatic electrons
 - Reduced guiding center's equation of motion: ρ^* terms omitted, only dominant magnetic drift velocity $\mathbf{v}_d = v_d \nabla Z$
 - Constant equilibrium n_i, B in ion polarization density perturbation (quasi-neutrality)
 - Single toroidal harmonic, Dirichlet B.C. for field, "absorbing" B.C. for markers
- PETSC library used as the field solver
- Runge-Kutta 4th order scheme of the particle-field system

Recap: particle positioning scheme in unstructured mesh

- Rectangular grids are used for particle positioning (deposition/gathering) in unstructured meshes
 1. Rectangular grids are generated (“boxes”)
 2. Box-triangle mapping is generated
 3. During particle deposition/gathering, the box containing the particle is first found and the triangle is identified



The box (red lines) size and its comparison with the triangle (black lines) size for different values of N_x (box # in R direction + 1)

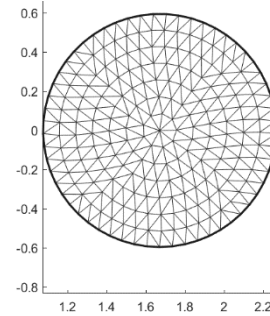


The speed-up of a medium size simulation ($N_r=90$, 25.6 million markers) for different values of N_x/N_r w.r.t. that with $N_x=2$ (1 box)

Recap: Ion Temperature Gradient mode simulations

- ITG simulation using Cyclone case shows reasonable agreement

- Differences are due to the simplifications in TRIMEG



- Tests in the whole plasma volume

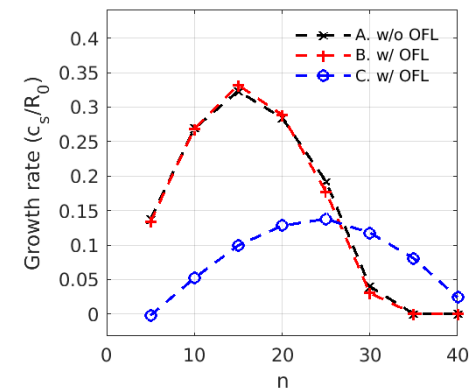
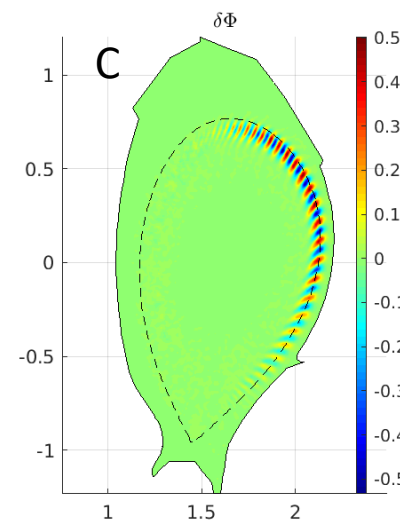
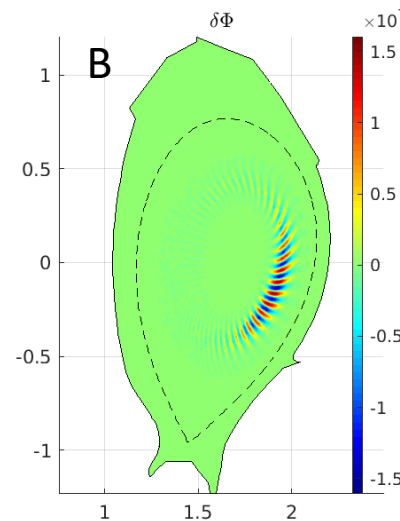
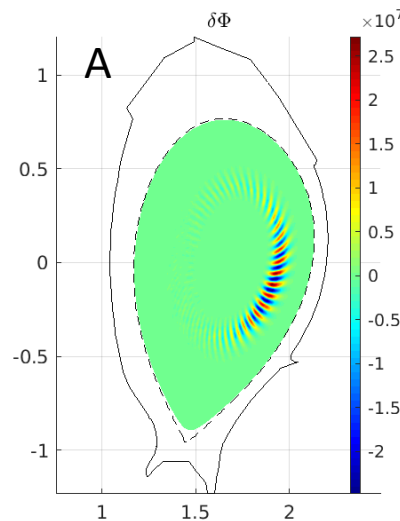
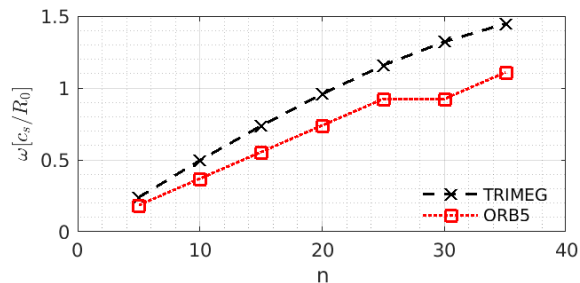
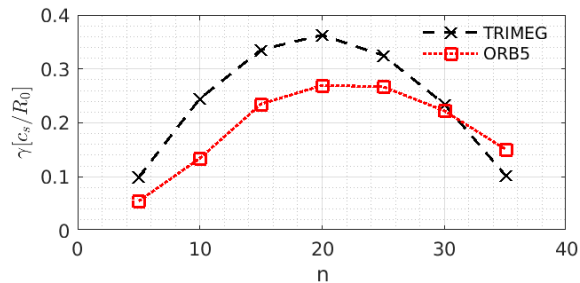
The 2D ITG mode structures (n=20) for:

Case A (left, w/o OFL, $\frac{d\ln T_i}{dr}$ peaks near $\psi = 0.25\psi_{edge}$)

Case B (middle, w/ OFL, $\frac{d\ln T_i}{dr}$ peaks near $\psi = 0.25\psi_{edge}$)

Case C (right, w/ OFL, $\frac{d\ln T_i}{dr}$ peaks near $\psi = \psi_{edge}$).

The dotted line indicates the separatrix.



Details in [Z.X. Lu, Ph. Lauber, T. Hayward-Schneider, A. Bottino, M. Hoelzl, *Phys. Plasmas*, [26, 122503 \(2019\)](#)]

Recap: limitation of the previous version of TRIMEG

- The simplified physics model, e.g., v_d , ρ^* terms (easier to fix), B.C., source & sink (more complicated) limits its application to realistic experiments
- TRIMEG(before 2019)
 - δf , electrostatic, explicit
 - Unstructured mesh
- This is part of the motivation to study the **full f, electromagnetic, implicit** scheme
- TRIMEG(since 2020)
 - Full f, electromagnetic, implicit
 - Structured mesh
 - Z.X. Lu, G. Meng, M. Hoelzl, Ph. Lauber, [arXiv:2007.06935](https://arxiv.org/abs/2007.06935) (2020)
 - Unstructured mesh in progress

Outline

- Background and motivation
- Focus of this work
 - Full f electromagnetic simulation and TRIMEG development
- From “particle enslavement” to “moment enslavement”
 - One dimensional model of shear Alfvén wave
 - Implicit scheme with “moment enslavement”
- Simulation of Alfvén waves in tokamak plasmas
 - Gyrokinetic equation and conservation properties
 - The mixed explicit-implicit scheme for electromagnetic simulations
 - Alfvén and EP simulations of ITPA case
- Conclusion and outlook, short messages

Models and equations (1D uniform plasma)

- Shear Alfvén wave in 1D uniform plasma [L. Chen, F. Zonca, *Rev. Modern Phys.* 88(1), 015008 and refs therein]
 - Ampere's law & quasi-neutrality (QN)

$$\nabla_{\perp}^2 \delta A_{\parallel} = -\mu_0 \delta j_{\parallel, e}$$

$$\nabla_{\perp} \cdot \left(\frac{nZ}{\omega_{c, s} B} \nabla_{\perp} \delta \phi \right) = \delta n_e - \delta n_i, Z: \text{charge \#}$$

- As dominant terms, the ion polarization density and δn_e balance each other in QN equation.
- Parallel electron motion:

$$\frac{dl}{dt} = v_{\parallel}; l: \text{parallel coordinate}$$

$$\frac{m}{e} \frac{dv_{\parallel}}{dt} = \partial_{\parallel} \delta \phi + \partial_t \delta A_{\parallel}$$

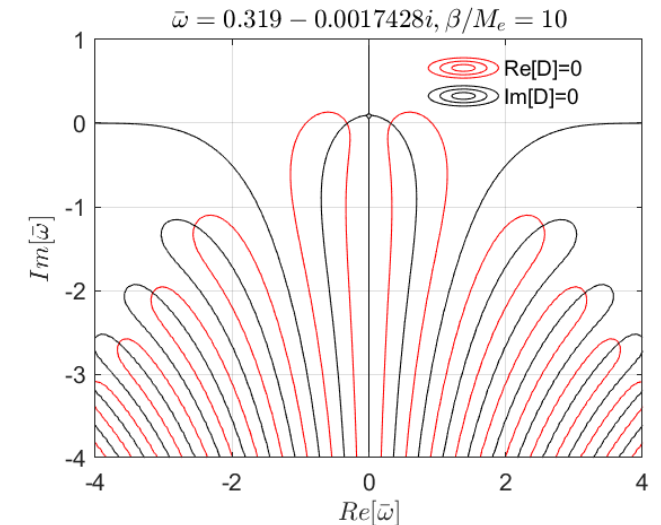
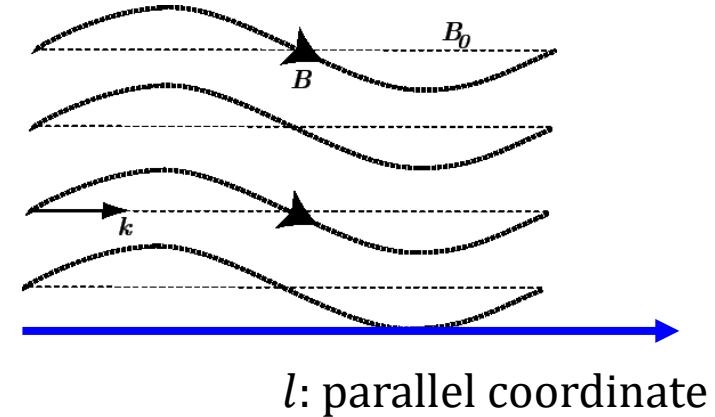
- Analytical dispersion relation ($\beta = v_{ti}^2/v_A^2$, v_{ti} , v_A : thermal, Alfvén velocities)

$$1 - \frac{2\beta[1+\bar{\omega}Z(\bar{\omega})]}{M_e(k_{\perp}\rho_{ti})^2} \left(\bar{\omega}^2 - \frac{M_e}{\beta} \right) = 0, \bar{\omega} = \omega/\omega_{te}, \omega_{te} = v_{te}k_{\parallel}$$

noticing Linearized GK equation in 1D uniform plasma ($f = f_0 + \delta f$):

$$\partial \delta f + v_{\parallel} \partial_{\parallel} \delta f = -\dot{v}_{\parallel} \partial_{v_{\parallel}} f_0$$

Light electrons response quickly along B and can destroy the simulation. The larger β/M_e is, the more difficult



The implicit scheme for the field-particle system

- Normalized equations

- Parallel electron motion (electrons):

$$\frac{dl}{dt} = v_{\parallel}; l: \text{parallel coordinate}$$

$$\frac{dv_{\parallel}}{dt} = \partial_{\parallel} \delta\phi + \partial_t \delta A_{\parallel}$$

- Ampere's law & quasi-neutrality

$$\nabla_{\perp}^2 \delta A_{\parallel} = C_A \delta J_{\parallel}$$

$$\nabla_{\perp} \cdot \left(\frac{B_0^2}{B^2} \nabla_{\perp} \delta\phi \right) = C_P \delta N$$

$$C_A = \beta / \rho_{tN}^2, C_P = 1 / \rho_{tN}^2$$

- Normalization units

$$R_N = 1m, v_N = \sqrt{2T_N/m_N}, \rho_{tN} = \frac{m_N v_N}{e B_0}$$

$$(\delta\phi, \delta A_{\parallel}, T) \text{ normalized to } \left(\frac{m_N v_N^2}{e}, \frac{m_N v_N}{e}, \frac{m_N v_N^2}{2} \right)$$

- Crank-Nicolson scheme (implicit)

$$\frac{l^{t+\Delta t} - l^t}{\Delta t} = \frac{v_{\parallel}^{t+\Delta t} + v_{\parallel}^t}{2}$$

$$\frac{v_{\parallel}^{t+\Delta t} - v_{\parallel}^t}{\Delta t} = \partial_{\parallel} \frac{\delta\phi^{t+\Delta t} + \delta\phi^t}{2} + \frac{\delta A_{\parallel}^{t+\Delta t} - \delta A_{\parallel}^t}{\Delta t}$$

$$\nabla_{\perp}^2 \delta A_{\parallel}^{t,t+\Delta t} = C_A \delta J_{\parallel}^{t,t+\Delta t}$$

$$\nabla_{\perp} \cdot \left(\frac{B_0^2}{B^2} \nabla_{\perp} \delta\phi^{t,t+\Delta t} \right) = C_P \delta N^{t,t+\Delta t}$$

- Total Degree of Freedom: $(N_G + N_p)$

- First simplification using “particle enslavement”: $(l, v_{\parallel})^{t+\Delta t}$ written as functions of $(\delta\phi, \delta A_{\parallel})^{t+\Delta t}$; then DOF reduced to N_G [G. Chen 2011]

- For large DOF in TRIMEG, we aim for even lower cost since field DOF $> 10^5$

- Second simplification: “moment enslavement” in this work

Procedure of the implicit particle-field solver

- Iterations start with an explicit solution at $i=1$, aiming for solution to C-N scheme

i : iteration #

$$\xrightarrow{1} \left\{ \begin{array}{l} \delta\Phi^{start}(t + \Delta t) \\ \delta A_{\parallel}^{start}(t + \Delta t) \end{array} \right\}^i \xrightarrow{2} \left\{ \begin{array}{l} l(t + \Delta t) \\ v_{\parallel}(t + \Delta t) \end{array} \right\}^i \xrightarrow{3} \left\{ \begin{array}{l} \delta N^{end}(t + \Delta t) \\ \delta J^{end}(t + \Delta t) \end{array} \right\}^i \xrightarrow{3} \left\{ \begin{array}{l} \delta\Phi^{end}(t + \Delta t) \\ \delta A_{\parallel}^{end}(t + \Delta t) \end{array} \right\}^i \xrightarrow{4} \left\{ \begin{array}{l} \delta\Phi^{start}(t + \Delta t) \\ \delta A_{\parallel}^{start}(t + \Delta t) \end{array} \right\}^{i+1}$$

1. Each iteration starts with the given field $\{F^{start}(t + \Delta t)\}^i$, where $F \equiv \{\delta\phi, \delta A_{\parallel}\}$
2. Push particles implicitly from t to $t + \Delta t$ (relatively easy).
3. In the end of each iteration, fields $\{F^{end}(t + \Delta t)\}^i$ are solved
4. Fields $\{F^{start}(t + \Delta t)\}^{i+1}$ are set so that $|\{F^{start}(t + \Delta t)\}^{i+1} - \{F^{end}(t + \Delta t)\}^{i+1}| \rightarrow 0$ in the next iteration.

Step 4: the proper estimate of the field $\{F^{start}(t + \Delta t)\}^{i+1}$ is the key of achieving good convergence

Analytic treatment in iteration: “moment enslavement”

- Particle enslavement: $l = l(\delta\phi, \delta A_{\parallel}), v_{\parallel} = v_{\parallel}(\delta\phi, \delta A_{\parallel})$
- Moment enslavement: $\delta N^{end} = \delta N^{end}(l, v_{\parallel}) = \delta N^{end}(\delta\phi, \delta A_{\parallel})$

i: iteration #

Step 4: analytic form for setting $\{F^{start}(t + \Delta t)\}^{i+1}: \{\delta\phi^{start}, \delta A_{\parallel}^{start}\}^{i+1} = \{\delta\phi^{end}, \delta A_{\parallel}^{end}\}^i + \{\Delta\delta\phi, \Delta\delta A_{\parallel}\}$, with

$$\left[\begin{pmatrix} \frac{1}{c_P} \nabla_{\perp}^2 & 0 \\ 0 & \frac{1}{c_A} \nabla_{\perp} \cdot \frac{B_0^2}{B^2} \nabla_{\perp} \end{pmatrix} - \bar{\bar{M}}_c \right] \cdot \begin{bmatrix} \Delta\delta\phi \\ \Delta\delta A_{\parallel} \end{bmatrix} = \begin{bmatrix} \delta N^{end} - \delta N^{start} \\ \delta J^{end} - \delta J^{start} \end{bmatrix}^i, \bar{\bar{M}}_c = \begin{bmatrix} \frac{\partial \delta N^{end}}{\partial \delta\phi} & \frac{\partial \delta N^{end}}{\partial \delta A_{\parallel}} \\ \frac{\partial \delta J^{end}}{\partial \delta\phi} & \frac{\partial \delta J^{end}}{\partial \delta A_{\parallel}} \end{bmatrix}$$

$(N_G + N_p)^2$ matrix inversion: unacceptable \rightarrow “particle enslavement” [G. Chen 2011]

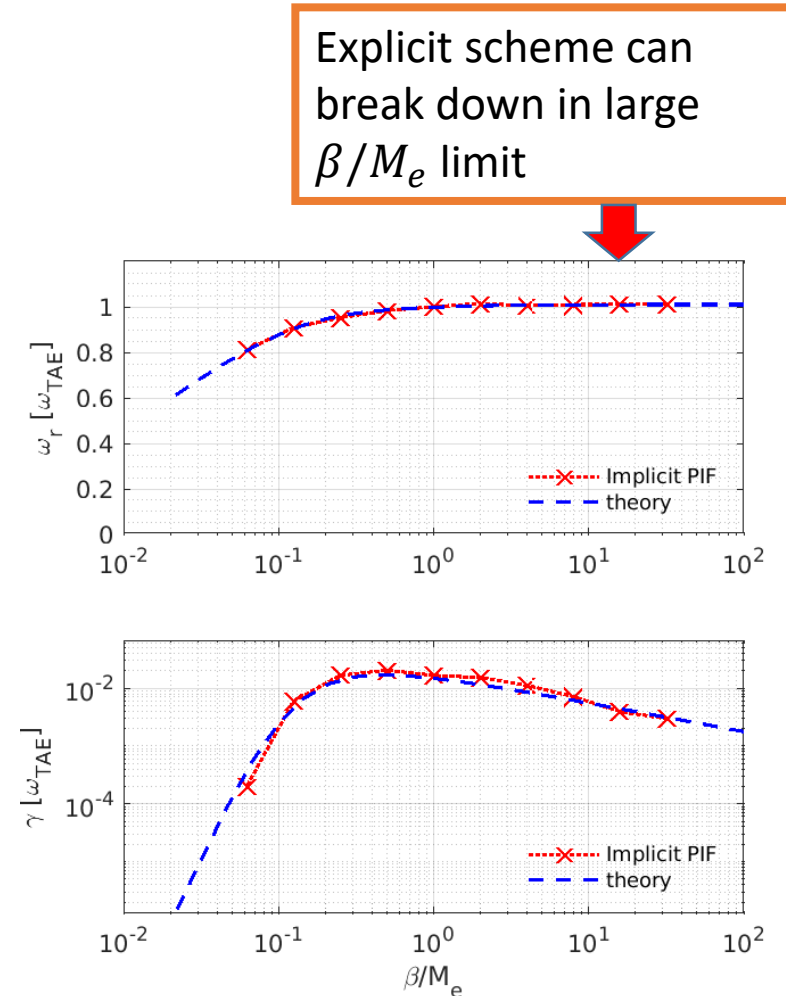
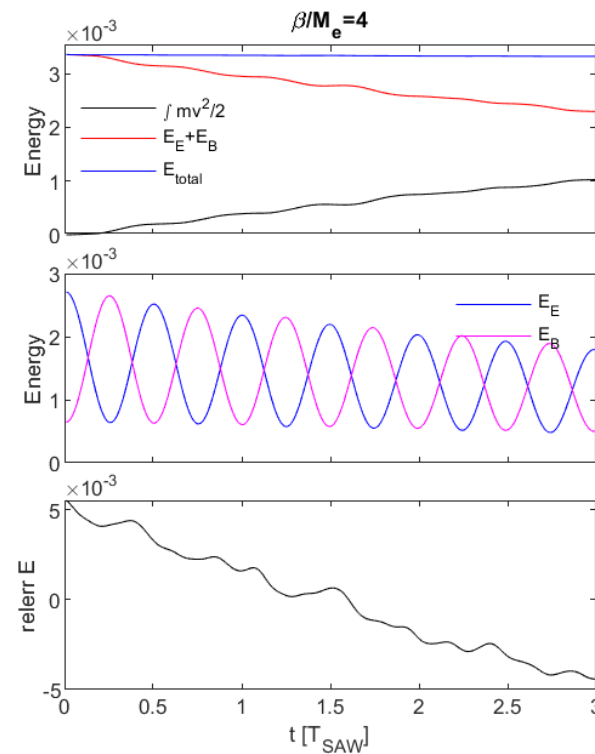
$$\bar{\bar{M}}_c \approx \begin{bmatrix} \frac{k_{\parallel}^2 \Delta t^2}{4M_e} & -i \frac{k_{\parallel} \Delta t}{2M_e} \\ i \frac{k_{\parallel} \Delta t}{2M_e} & \frac{1}{M_e} \end{bmatrix} \text{ obtained analytically; rigorous form more complicated but can be implemented}$$

Another way: push particles and calculate $\bar{\bar{M}}_c$; more expensive by a factor of N_p , i.e., particle number.

$\bar{\bar{M}}_c$ calculation ($N_G \times N_p$): not cheap \rightarrow analytic acceleration here, i.e., “moment enslavement”

1D SAW simulations

- The implicit scheme is capable of simulating SAW in a broad range of β/m_e
 - The relative error in total energy is below 5×10^{-3}
 - Damping rate and real frequency properly simulated
- $k_{\perp} \rho_N = 0.2$, $\frac{\beta}{M_e} \in \left[\frac{1}{16}, 32 \right]$, marker # $N_p = 10^5$, $dt = 0.01 T_{SAW}$, ρ_N : ion Larmor radius
Parameters are relevant to tokamak plasmas, e.g., $\beta = 1\%$, $M_e = 1/1836$, $\frac{\beta}{M_e} = 18.36$
- For high β/M_e , it takes more iterations to achieve good convergence.
 - The challenge in high β/M_e corresponds to the “cancelation” problem in p_{\parallel} formula.
 - Using the implicit scheme, the SAW can be simulated for high β/M_e , although more expensive



Details in [Z.X. Lu, G. Meng, M. Hoelzl, Ph. Lauber, [arXiv:2007.06935](https://arxiv.org/abs/2007.06935) (2020)]

Outline

- Background and motivation
- Focus of this work
 - Full f electromagnetic simulation and TRIMEG development
- From “particle enslavement” to “moment enslavement”
 - One dimensional model of shear Alfvén wave
 - Implicit scheme with “moment enslavement”
- **Simulation of Alfvén waves in tokamak plasmas**
 - Gyrokinetic equation and conservation properties
 - The mixed explicit-implicit scheme for electromagnetic simulations
 - Alfvén and EP simulations of ITPA case
- Conclusion and outlook, short messages

Conservation properties of particle motion

- Conservation of particle energy and toroidal canonical momentum in equilibrium

$$\frac{d\mathbf{R}}{dt} = v_{\parallel} \mathbf{b} + \mathbf{v}_d, \quad \mathbf{v}_d = \frac{m_s}{e_s B^2} (v_{\parallel}^2 + \mu B) \mathbf{b} \times \nabla B;$$

$$\frac{dv_{\parallel}}{dt} = -\mu \partial_{\parallel} B; \text{ ignoring } \rho^* \equiv \rho/L \text{ higher order terms}$$

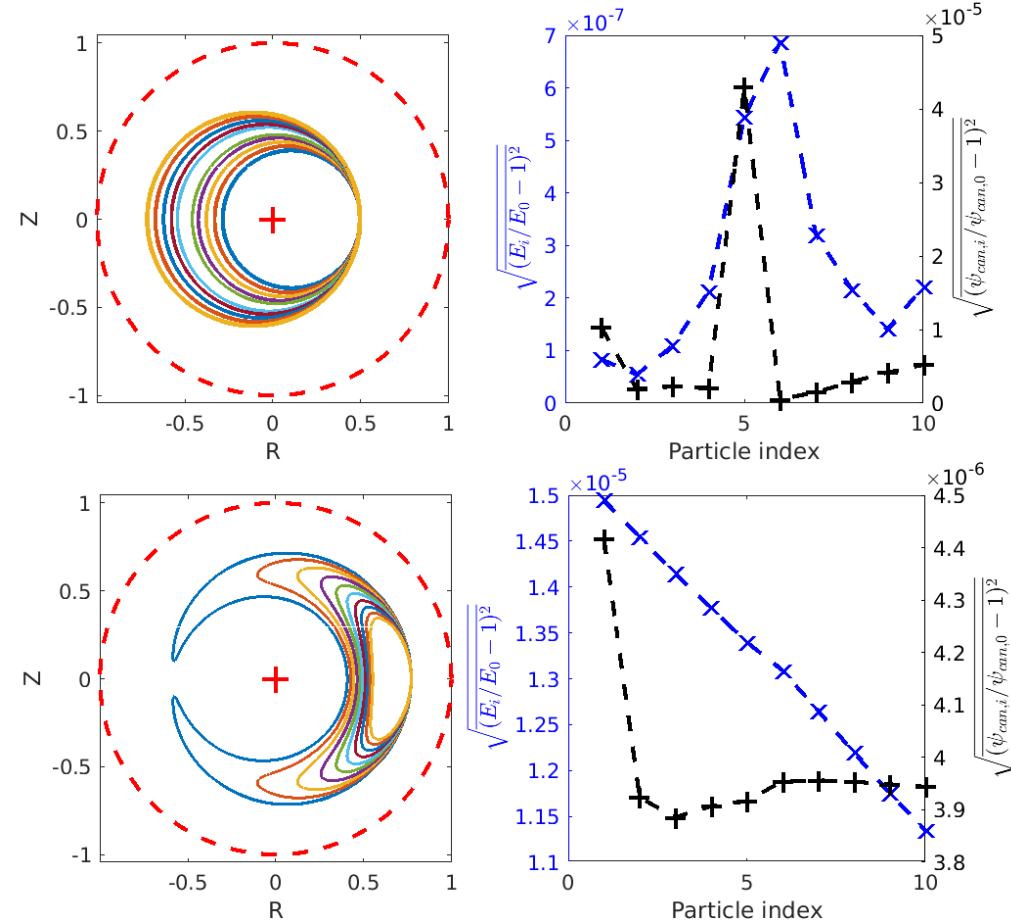
- With $P_{\phi} \equiv e_s \psi + m v_{\parallel} F/B$, $E = \mu B + v_{\parallel}^2/2$,

$$\frac{dP_{\phi}}{dt} = 0, \quad \frac{dE}{dt} = 0 \text{ can be proved in equilibrium}$$

- Comprehensive form (with ρ^* corrections) not adopted for simpl

- Fourth order Runge-Kutta integral of particle trajectory gives low relative error

- Low relative error ($\sim 10^{-5}$) for similar parameters in TAE simulations
- Particle temperature: 400 keV (energetic particles), $v_{ts} = \sqrt{2T_s/m_s}$.
- For passing particles (the upper row), $\mu = 0.04v_{ts}^2$, $v_{\parallel} \in [-2v_{ts}, 2v_{ts}]$, $0.5, \theta = 0$.
- For trapped particles (the lower row), $\mu \in [0.15v_{ts}^2, v_{ts}^2]$, $v_{\parallel} = -0.2v_{ts}$ at $r = 0.8, \theta = 0$.



Mixed explicit (Runge-Kutta)-implicit scheme in torus

- Treat **fast parallel particle motion implicitly** but **perpendicular one and slow || motion explicitly**

$$\frac{d\mathbf{R}}{dt} = \mathbf{v}_{\parallel} \mathbf{b} + \mathbf{v}_d + \frac{\mathbf{b}}{B} \times \nabla(\delta\phi - v_{\parallel} \delta A)$$

$$\frac{dv_{\parallel}}{dt} = -\mu \partial_{\parallel} B - \frac{e_s}{m_s} (\partial_{\parallel} \delta\phi + \partial_t \delta A)$$

- It is possible to treat all terms implicitly (more complicated)
- ρ^* terms ignored in the present version; single n
- Ion: only polarization density for most runs
- EP, electrons: Gyrokinetic (w/o FLR)

- Inspired by the theoretical “mixed WKB-full-wave approach” [Zonca, *Phys. Fluids B* 5, 3668 (1993); Lu, *Phys. Plasmas*, [19 \(4\), 042104 \(2012\)](#)].

- Equilibrium particle motion (**explicit**)

$$\frac{d\mathbf{R}_0}{dt} = \mathbf{v}_d + \frac{\mathbf{b}}{B} \times \nabla(\delta\phi - v_{\parallel} \delta A)$$

$$\frac{dv_{\parallel 0}}{dt} = -\mu \partial_{\parallel} B$$

- Perturbed particle motion (**implicit**)

$$\frac{d\mathbf{R}_1}{dt} = v_{\parallel} \mathbf{b}$$

$$\frac{dv_{\parallel 1}}{dt} = -\frac{e_s}{m_s} (\partial_{\parallel} \delta\phi + \partial_t \delta A)$$

- Runge-Kutta 4th order implemented

Numerical convergence: field solver

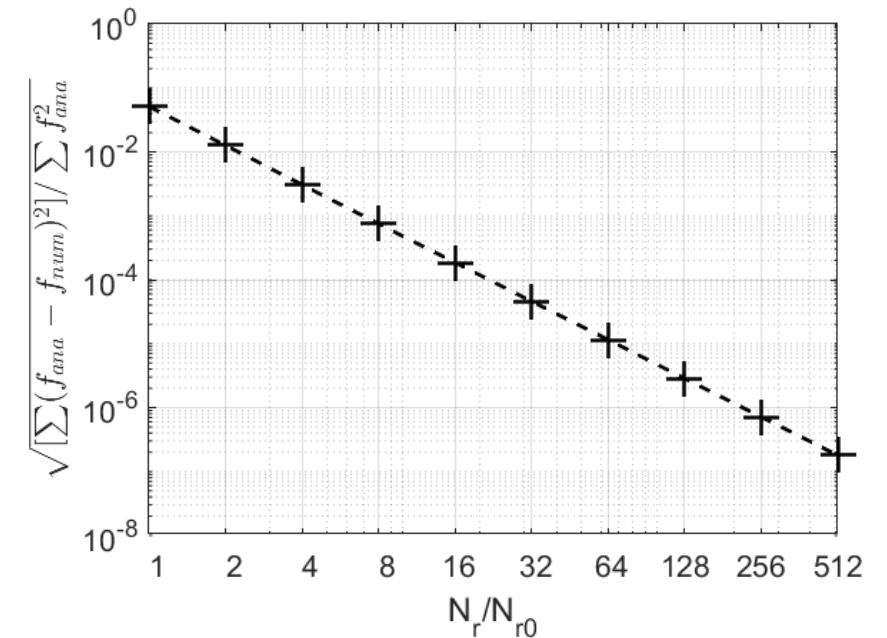
- The field solver is tested using the Method of Manufactured Solutions (MMS)
 - Fourier decomposition in θ, ϕ directions; linear finite element in radial direction
 - The Poisson and the Ampère solvers are both constructed from the mass and stiffness matrices, corresponding to ∂_r^2, ∂_r and equilibrium variables $f(r)$. As a result, testing the Ampère solver is sufficient for the numerical verification of the basic field operators.

- Analytic solutions to $\left(\frac{\partial^2}{\partial r^2} + \frac{1}{r} \frac{\partial}{\partial r} - \frac{m^2}{r^2}\right) \delta A_{\parallel, m} = C_A \delta J_m$

$$\delta A_{\parallel, m, ana} = c_0 + c_1 r + a_J J_m(r) + e^{-\frac{(r-r_c)^2}{W^2}},$$

$$C_A \delta J_{m, ana} = a_2 r^2 + a_3 r^3 + a_+ r^m + a_- r^{-m} - a_J J_m(r) + e^{-\frac{(r-r_c)^2}{W^2}} \times \left[\frac{4(r-r_c)^2}{W^4} - \frac{2}{W^2} - \frac{2(r-r_c)}{rW^2} - \frac{m^2}{r^2} \right], \text{ Bessel function } J_m.$$

- Numerical test: use $C_A \delta J_{m, ana}$ as input and solve for $\delta A_{\parallel, m, num}$;
estimate the relative error $\sqrt{\left[\sum_k \left(f_{num, k} - f_{ana}(r_k) \right)^2 \right] / \sum_k f_{ana}^2(r_k)}$
- Reasonable convergence v.s. grid number observed in the figure.



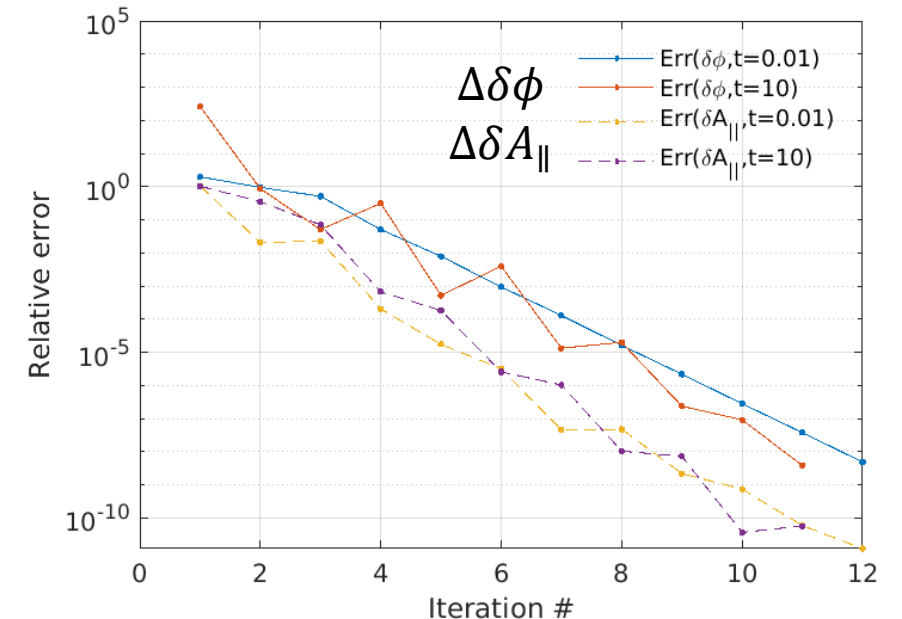
Numerical convergence: implicit field-particle solver

- In order to test the convergence of the implicit field-particle solver, the relative correction in $\delta\phi$ and δA_{\parallel} in every iteration are analyzed

$$\xrightarrow{1} \left\{ \begin{array}{l} \delta\Phi^{start}(t + \Delta t) \\ \delta A_{\parallel}^{start}(t + \Delta t) \end{array} \right\}^i \xrightarrow{2} \left\{ \begin{array}{l} l(t + \Delta t) \\ v_{\parallel}(t + \Delta t) \end{array} \right\}^i \xrightarrow{3} \left\{ \begin{array}{l} \delta N^{end}(t + \Delta t) \\ \delta J^{end}(t + \Delta t) \end{array} \right\}^i \xrightarrow{3} \left\{ \begin{array}{l} \delta\Phi^{end}(t + \Delta t) \\ \delta A_{\parallel}^{end}(t + \Delta t) \end{array} \right\}^i \xrightarrow{4} \left\{ \begin{array}{l} \delta\Phi^{start}(t + \Delta t) \\ \delta A_{\parallel}^{start}(t + \Delta t) \end{array} \right\}^{i+1}$$

- In Step 4: set the field for the next iteration, $\{\delta\phi^{start}, \delta A_{\parallel}^{start}\}^{i+2} = \{\delta\phi^{end}, \delta A_{\parallel}^{end}\}^{i+1} + \{\Delta\delta\phi, \Delta\delta A_{\parallel}\}$
- As $\{\Delta\delta\phi, \Delta\delta A_{\parallel}\} \rightarrow 0$, the implicit solution of the particle-field system is obtained
- Convergence to machine precision observed ($\sim 10^{-16}$ or 10^{-31})
- $\{\Delta\delta\phi, \Delta\delta A_{\parallel}\}$ during the first several iterations can be $\sim O(1)$.

This is typical for high β/M_e cases. Without this correction, simulation crashes



The convergence of $\delta\phi$ and δA_{\parallel} at the beginning ($t = 0.01T_{TAE}$) and the end ($t = 10T_{TAE}$) of EP driven TAE case₂₀

Simulation of SAW and EP physics using ITPA parameters

- A widely benchmarked case is chosen as a test [Könies et al Nucl. Fusion 58 (2018) 126027]
- Equilibrium: $R_0 = 10m$, $a = 1m$, $q = 1.71 + 0.16r^2$, $B_0 = 3T$
- Uniform thermal ion & electron temperature & density profiles, $T_e = T_i = 1keV$,
 $n_e = n_i = 2 \cdot 10^{19}/m^3$
- Energetic particles (EPs): density gradient drives the mode (constant T_{EP})

$$n(r) = n_{f0} c_3 \exp \left\{ -\frac{c_2}{c_1} \tanh \frac{r-c_0}{c_2} \right\}, \quad \begin{array}{l} n_{f0} = 1.44131 \cdot 10^{17} m^{-3}, c_0 = 0.49123, \\ c_1 = 0.298228, c_2 = 0.198739, c_3 = 0.521298 \end{array}$$

- More simplifications in this work: only polarization density kept for thermal ions

Electron Landau damping of SAW

- Wave-particle interaction properly simulated by calculating the electron Landau damping

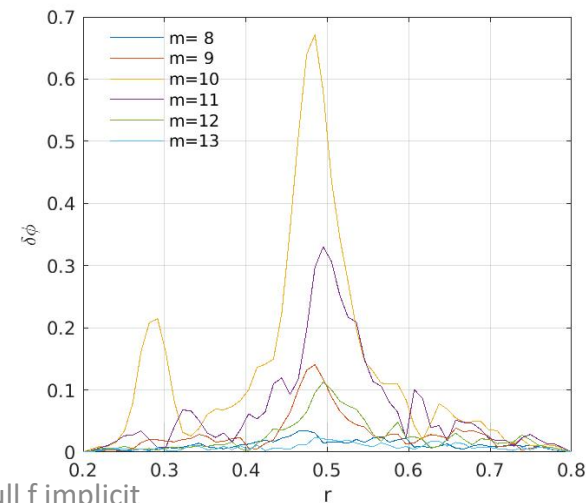
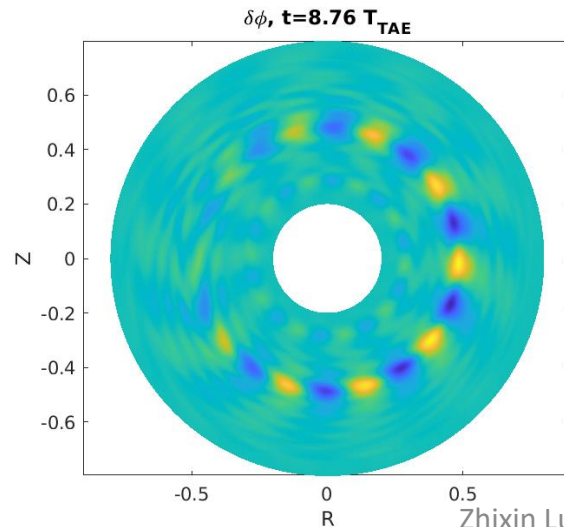
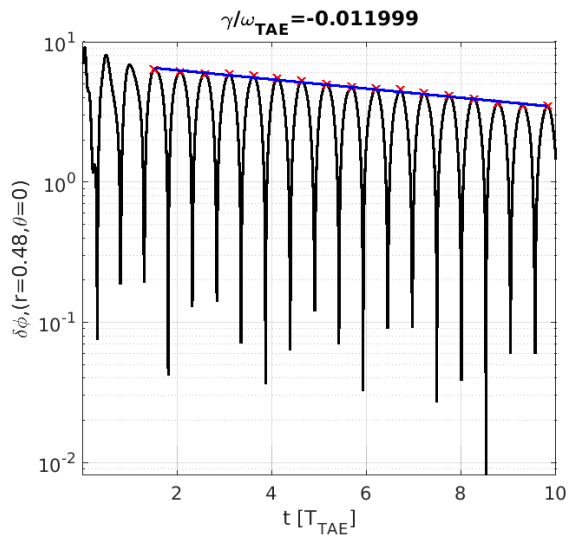
- The Gaussian shape $\exp\left\{-\frac{(r-r_{pc})^2}{W_p^2}\right\}$ of the density perturbation is set to be as close as possible to the TAE eigenmode, with $W_p = 0.025$, $r_{pc}(m = 10) = 0.47$, $r_{pc}(m = 11) = 0.51$.

γ/ω_r	$\frac{m_i}{m_e} = 200$	$\frac{m_i}{m_e} = 1836$
LIGKA	-1.293%	-0.5000%
TRIMEG	-1.248%	-0.5008%

Other parameters: marker #:

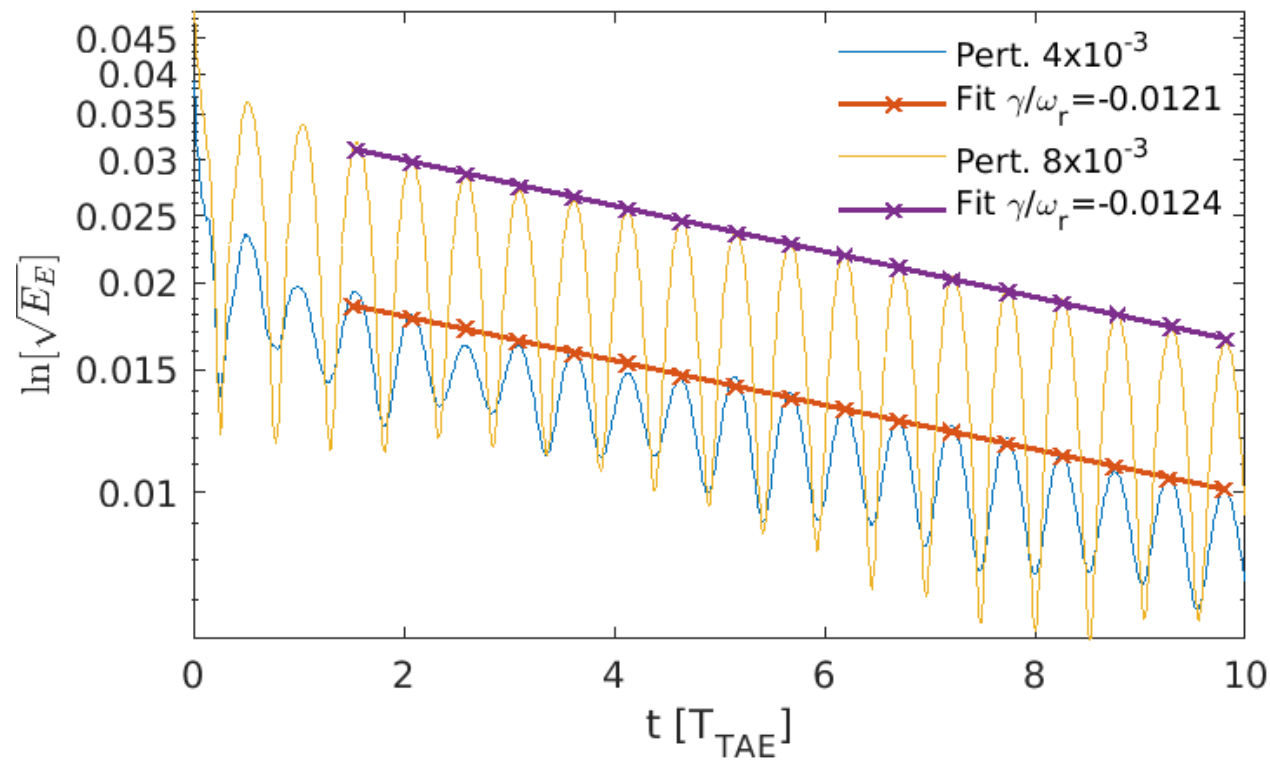
16e6 electrons, $\frac{m_i}{m_e} = 200, 1836$,

on 320 Intel Xeon Gold 6148 processors for 10 or 80 hours



Linear Landau damping (w/o energetic particles)

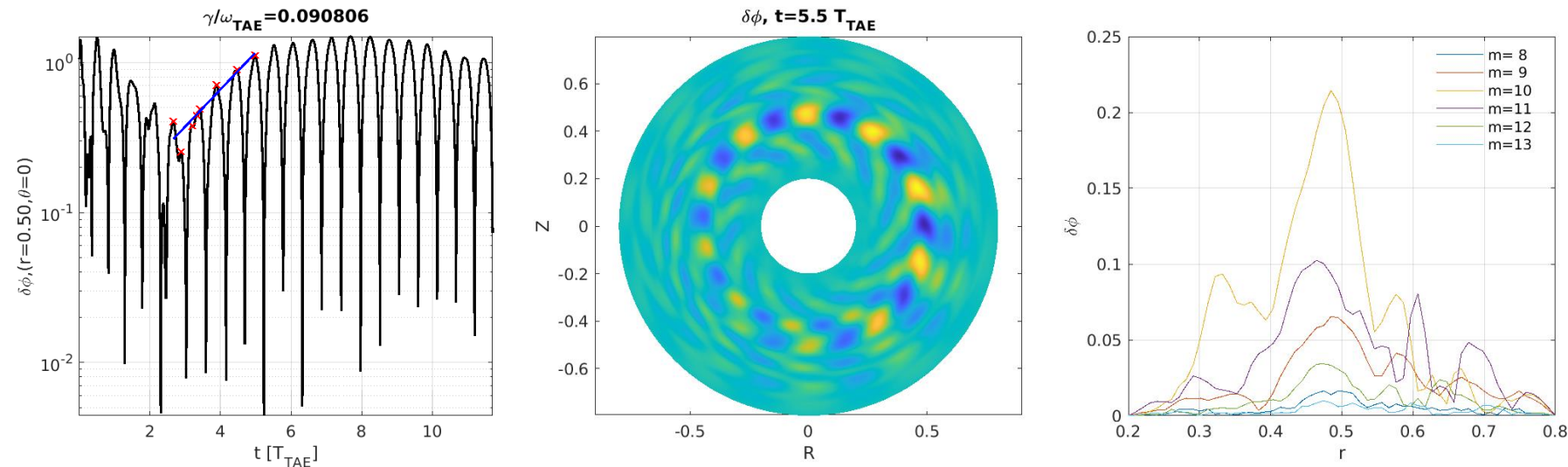
- Initial perturbation small enough for linear Landau damping test
 - In small perturbation limit, the damping rate converges towards the linear results



Excitation of EP driven TAE

- Clear mode destabilization observed, with reasonable γ/ω_r produced
 - Markers #: 128e6 electrons, 32e6 EPs, $\frac{m_i}{m_e} = 200$, on 960 processors for 36 hours
 - Mode radial width (FWHM) $\Delta r \approx 0.12$, larger than that in TAE damping case ($\Delta r \approx 0.06$). It's due to the EP's non-perturbative effects on mode width

[Lu Nucl. Fusion 58 (2018) 082021 and refs. therein]



Details in [Z.X. Lu, G. Meng, M. Hoelzl, Ph. Lauber, [arXiv:2007.06935](https://arxiv.org/abs/2007.06935) (2020)]

Zhixin Lu, full f implicit

Conclusions and outlook

- The implicit scheme has been implemented for the full f electromagnetic simulations of Alfvén waves and EP physics.
 - Using the [analytical derivation based implicit scheme](#), good convergence of the field-particle solver is demonstrated
 - By applying to the 1D shear Alfvén wave problem, this implicit scheme shows good energy conservation and capabilities of calculating the frequency and damping rate properly [in a broad range of \$\beta/M_e\$](#) values, including the small electron mass condition
 - The application of this method to the TAE problem shows its [applicability for electromagnetic simulations](#) with/without EPs. The TAE mode structure distortion due to the non-perturbative effects of the EPs is observed, consistent with previous simulations and theoretical studies
- More efforts needed for more comprehensive model
 - While the mixed implicit-explicit scheme has been implemented, its connection to the fully implicit scheme needs to be tested
 - The application to the unstructured mesh enables simulation in the whole tokamak volume and merits more efforts

Short remarks from this work

- Specific issues addressed in this work

Q: What's the **minimum cost** of implicit scheme, especially when field **DOF is $>10^5$** (typical DOF in unstructured mesh FEM solver)?

Remark: With “**moment enslavement**”, cost of implicit solver can be further reduced during field correction, from $N_p N_G$ to N_G in calculating $\bar{\bar{M}}_c = \left[\frac{\partial \delta N^{end}}{\partial \delta \phi}, \frac{\partial \delta N^{end}}{\partial \delta A_{\parallel}}; \frac{\partial \delta J^{end}}{\partial \delta \phi}, \frac{\partial \delta J^{end}}{\partial \delta A_{\parallel}} \right]$

Q: Is the implicit scheme useful for mitigating “**cancellation problem**” or for simulations with **realistic ion to electron mass ratio**?

Remark: for v_{\parallel} formula, numerical problem in $\partial A / \partial t$ is mitigated, if compared with pure RK4 scheme (crash), for ITPA case.

Implicit scheme enables simulation using realistic m_i / m_e . It takes more iterations if lighter electrons is included.

Comparison with Pullback or control variate schemes merits more efforts.

Implicit scheme for p_{\parallel} formula in progress.

Also: mixed pullback-implicit scheme [A. Mishchenko, et al., Comput. Phys. Commun. 238, 194 (2019)]?

Q: What are the technical **pros and cons** of the fully implicit scheme?

Remark: pros: conservation & larger time step size in some cases (tested in 1D electrostatic case)

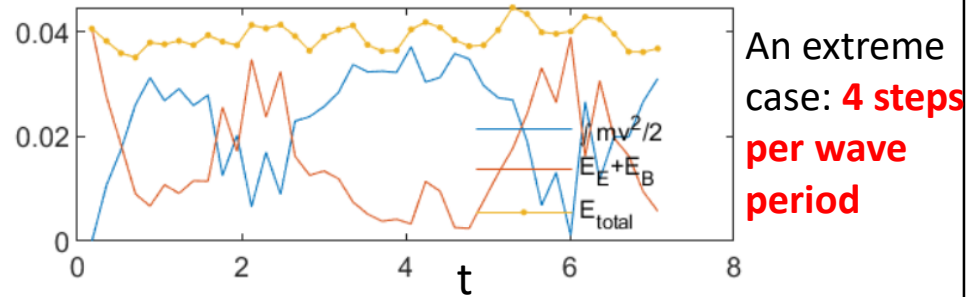
cons: additional solvers needed with **matrix size 2X** of the Poisson or Ampere solver, iteration needed (minor cons); fully implicit scheme is more complicated than mixed implicit-explicit one (moderate cons)

Q: Any reasonable balance point between physics studies and numerical capabilities, such as **mixed implicit-explicit scheme**?

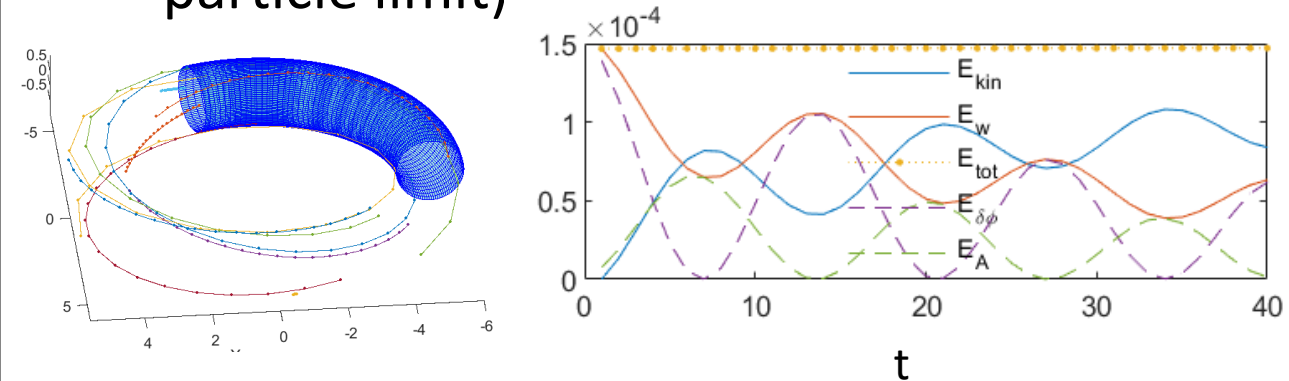
Remark: Yes. With the **mixed scheme**, it's possible to run some realistic physics cases (ITPA TAE).

Four steps of implicit full f scheme development in TRIMEG

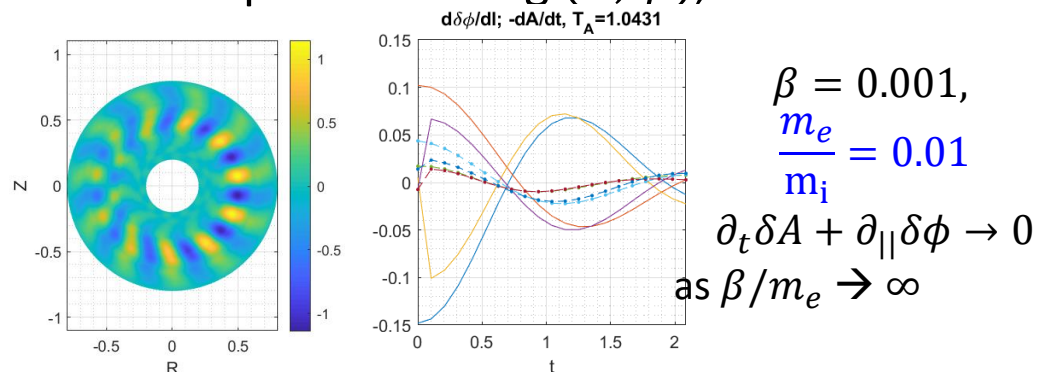
- 1D case, gyrokinetic electrons
 - Shear Alfvén wave, SAW (done)
 - Current driven mode (to do)



- 2D Single flux surface (cylinder limit)
 - Shear Alfvén wave simulated (well passing particle limit)



- 3D circular geometry (tokamak)
 - Finite element method along r , Fourier decomposition along (θ, ϕ) ; PIC-PIF-PIF



- Present focus: realistic tokamak

- Goal: electromagnetic, full f, implicit, kinetic e^- model
- Realistic tokamak geometry
- Simulation of kinetic ballooning mode

